AD-A113 471 ARIZONA UNIV TUCSON DEPT OF CHEMISTRY F/G 20/6
THEORY AND EVALUATION OF A WINDOWLESS NON-RESONANT OPTOACOUSTIC--ETC(U)
DEC 81 S B TILDEN, M B DENTON N00014-75-C-0513
UNCLASSIFIED TR-30 NL

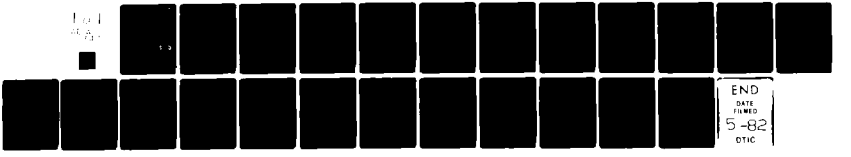

END
DATE FILMED
5-82
DTIC

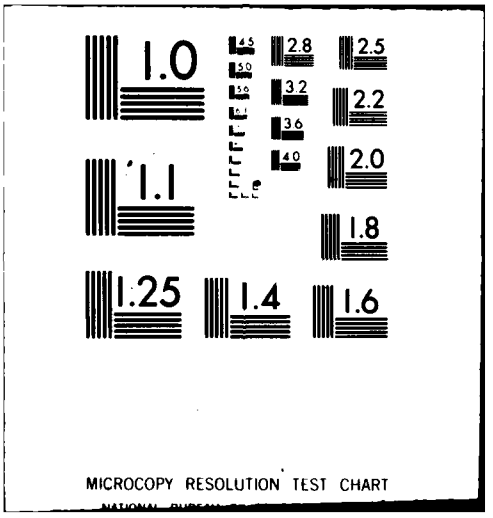
1.0
1.1
1.25
1.4
1.6
1.8
2.0
2.2
2.5
2.8
3.2
3.6
4.0
4.5
5.0
5.6
MICROCOPY RESOLUTION TEST CHART

SECURITY CLASSIFICATION OF THIS PAGE (When Data Entered)

12

REPORT DOCUMENTATION PAGE

READ INSTRUCTIONS BEFORE COMPLETING FORM

1. REPORT NUMBER: 30	2. GOVT ACCESSION NO.: AD-A113 471
	3. RECIPIENT'S CATALOG NUMBER:
4. TITLE (and Subtitle): Theory and Evaluation of A Windowless Non-Resonant Optoacoustic Cell	5. TYPE OF REPORT & PERIOD COVERED: Interim
	6. PERFORMING ORG. REPORT NUMBER:
7. AUTHOR(s): Scott B. Tilden and M. Bonner Denton	8. CONTRACT OR GRANT NUMBER(s): N00014-75-C-0513
9. PERFORMING ORGANIZATION NAME AND ADDRESS: Department of Chemistry, The University of Arizona, Tucson, Arizona 85721	10. PROGRAM ELEMENT, PROJECT, TASK AREA & WORK UNIT NUMBERS: NR 051-549
11. CONTROLLING OFFICE NAME AND ADDRESS: Office of Naval Research, Arlington, Virginia 22217	12. REPORT DATE: December 1, 1981
	13. NUMBER OF PAGES: 20
14. MONITORING AGENCY NAME & ADDRESS (if different from Controlling Office)	15. SECURITY CLASS. (of this report): Unclassified
	15a. DECLASSIFICATION/DOWNGRADING SCHEDULE:

16. DISTRIBUTION STATEMENT (of this Report)

Approved for public release; distribution unlimited

17. DISTRIBUTION STATEMENT (of the abstract entered in Block 20, if different from Report)

DTIC ELECTE S APR 15 1982 D

18. SUPPLEMENTARY NOTES

Prepared for publication in Applied Spectroscopy

19. KEY WORDS (Continue on reverse side if necessary and identify by block number)

Optoacoustic Spectrometry, Optoacoustic Cell, Windowless Cell

20. ABSTRACT (Continue on reverse side if necessary and identify by block number)

A novel non-resonant flow-through optoacoustic cell is characterized. This cell is operated without windows, completely eliminating the window background interference. Data are presented comparing sensitivity, resistance to cross-contamination, and operating characteristics of this approach with more conventional single and differential cell techniques. The capability of operation at widely varying sample flow rates is demonstrated.

DD FORM 1 JAN 73 1473 EDITION OF 1 NOV 65 IS OBSOLETE S/N 0102-LF-014-6601

SECURITY CLASSIFICATION OF THIS PAGE (When Data Entered)

AD A113471

DTIC FILE COPY

OFFICE OF NAVAL RESEARCH

Contract N00014-75-C-0513

Task No. NR 051-549

TECHNICAL REPORT NO. 30

Theory and Evaluation of

A Windowless Non-Resonant Optoacoustic Cell

by

Scott B. Tilden and M. Bonner Denton

Department of Chemistry
University of Arizona
Tucson, Arizona 85721

Prepared for Publication
in
Applied Spectroscopy

12/10

THEORY AND EVALUATION OF

A WINDOWLESS NON-RESONANT OPTOACOUSTIC CELL

Scott B. Tilden

and

M. Bonner Denton

Department of Chemistry
The University of Arizona
Tucson, Arizona 85721

ABSTRACT

A novel non-resonant flow-through optoacoustic cell is characterized. This cell is operated without windows, completely eliminating the window background interference. Data are presented comparing sensitivity, resistance to cross-contamination, and operating characteristics of this approach with more conventional single and differential cell techniques. The capability of operation at widely varying sample flow rates is demonstrated.

Index Heading: Windowless Non-Resonant Flow-through Optoacoustic Cell.

THEORY AND EVALUATION OF A WINDOWLESS NON-RESONANT OPTOACOUSITC CELL

Interest in optoacoustic spectroscopy has had a resurgence due to the techniques' theoretical promise as an approach capable of detecting trace gases at the part-per-billion level.[1] However, it was soon realized that in order to reach this detection level, the large window background signal observed in conventional optoacoustic cells needed to be minimized.[2] Cell designs that have been successfully used to minimize this background signal include the differential cell,[3,4] multipass cell,[5,6] and windowless resonant cell.[7,8] Although these cell designs can reduce the window background to an acceptable level, all have certain limitations to their usefulness.

The window background signal in optoacoustic spectroscopy arises whenever a modulated light source passes through any window material. With the basic experimental arrangement shown in Figure 1, window background is generated from the two windows at each end of the optoacoustic cell. This signal is thought to be generated at the window-gas interfacial region, with the magnitude of this signal dependent on the heat capacity of the window material.[9] Given the choice of window materials useful in the IR region (sapphire, germanium, ZnSe, NaCl, KCl, etc.), all have similar heat capacities making the window background problem ubiquitous.

The differential cell, proposed first by Luft[3] and more recently by Deaton,[4] was historically the first attempt at a cell designed to minimize window background. This design incorporates two identical cells back-to-back with a connecting window between the two cells as shown in Figure 2. For this cell design to work properly, the two cells must be matched such that the background signal in one cell is identical with the other.

Background signal reductions of two orders of magnitude have been reported using this approach. However, special precautions against cell contamination must be observed since certain gas molecules (especially polar molecules) can be adsorbed on the cell walls. Adsorbed gas molecules in the analysis cell can then be released during subsequent analysis giving an uncorrected background signal.

The capability of analyzing very small volumes in the differential cell is one important advantage over other cell designs. This cell is amenable to off-site analysis where a remote sample is collected and subsequently injected into the cell. This advantage is shared with the multipass resonant cell.

The multipass cell [5,6] is another cell design which has shown promise in reducing the window background. These cells, usually of resonant design, incorporate multiple passes of the laser beam between windows mounted at each end of the cell. Since the laser beam passes through the window material only once, the effective signal to window background ratio is increased by the number of internal reflections in the cell cavity. As many as 20 internal reflections have been achieved in such a cell, giving an effective signal to background improvement of 20 over a conventional cell.

The multipass cell also has limitations. Since the cell must support many internal passes, the cell itself has a correspondingly larger diameter than that of single pass non-resonant cells. This introduces a loss of signal which is usually compensated by employing resonant operation. Maintaining resonance in an optoacoustic cell can be difficult, especially considering that a 1 degree K change in temperature of a resonant cell of a Q of 500 will decrease the optoacoustic signal by a factor of two.[2] Obviously

maintaining necessary temperature control can be difficult in many experimental situations. This introduces the need to operate the light chopper in a feedback mode with the optoacoustic signal to maintain optimum chopping frequency.

The multipass cell can also be very sensitive to impurities, especially when these impurities adsorb on the cell mirror faces. For optimum performance, the mirrors must be very highly reflective, otherwise each reflection off a mirror face can itself add to the background signal, negating the multipass advantage. Impurities such as vacuum pump oil and other vapors that form films can significantly decrease the reflectivity of mirror surfaces used in the IR region.

The windowless resonant cell proposed by Bruce et al. has also been shown to be effective in reducing the window background signal.[7] This cell employs an outer chamber with windows surrounding an inner resonant cavity. Baffles were placed between the outer windows and the inner resonant cavity to suppress the background signal from the outer window. It should be noted that this cell is windowless only in the sense that windows are absent from the inner resonant cavity, although the authors do seem to indicate that the cell can be used without windows. No data concerning the completely windowless operation was given. A resonant cell built by Kritchman, Shtrikman and Slatkine[8] did give data using a windowless configuration. This cell used the lowest order longitudinal acoustic resonant mode of a narrow open tube surrounded by a large external chamber to generate the optoacoustic signal. Windowless data were taken by introducing a large quantity of ethylene into the laboratory (initially at 20 ppm) and allowing gas to diffuse into the cell. A working curve from 20 ppm to 50 ppb of ethylene gas was presented based on exponential removal of ethylene by the air handling system. This gave a

detection limit of 50 ppb of ethylene. The background room noise was measured at 50 db (A weighting) while these data were measured. Flushing the cell in the windowless configuration was observed to introduce a serious noise source making this design unsuitable for flow-through operation and prone to cross contamination and memory effects.

Theory

A possible solution to the window background problem would be to eliminate the windows in a non-resonant cell altogether. However, in conventional non-resonant cells this is not possible due to the need to confine the pressure wave in the cell such that this energy can be used to move the diaphragm of the microphone. Except for an infinitely sensitive microphone, more energy is expended moving the diaphragm than is used to vent the pressure wave out of the cell.

It is also possible, however, to dynamically contain the pressure wave in the cell without the use of windows. The motivation for building the cell was to design a long path length cell which would minimize background in direct relation to the relative length increase over a shorter cell.[10] However, it is possible to remove the windows completely from the cell if the pathlength is sufficiently long in relation to the chopping frequency.

The theory of operation of this cell can best be explained by reference to Figure 3. Assume that the chopping rate is 1Khz. Although excitation takes place along the total bore of the cell, assume as a first approximation that excitation takes place in the center one third of the cell. During the half cycle when the beam is blocked, the pressure wave moves in both directions towards the end of the cell. However, since this half cycle is only 0.5 ms long, the pressure wave can only move 16.5 cm down the cell,

given the speed of propogation of a pressure wave in air at STP is approximately 34 X 10^3 cm/sec. During the next half cycle, with the laser again exciting along the bore of the cell, the previous pressure pulse moves another 16.5 cm but has not yet exited the cell. At the same time another pressure pulse is produced which is now contained by the previous pressure wave. Note that the pressure pulses are dynamically contained in the cell without the use of windows.

Experimental

The windowless non-resonant cell (Figure 4) is constructed of a 90 cm X 1.27 cm OD extruded aluminum tube with a wall thickness of 0.159 cm. The tube was perforated along the center one-half length with four rows of 30 (0.3 cm dia.) holes spaced 1.27 cm apart. Each row of holes was 90 degrees from the row adjacent to it. An aluminized myler sheath (mylar-A, 3 mils thick) 50 cm long was wrapped around this center region, keeping the distance between the aluminum tube and the sheath at 0.15 cm by plastic spacers at each end of the sheath. A one eighth inch "Swage-lok" fitting was epoxied 19 cm from one end of the cell at an angle of 55 degrees from perpendicular, pointing towards the longer end of the cell. This assured that the total length of the cell would be evenly flushed. A biasing connection was added to one end of the mylar sheath using conducting epoxy to assure electrical conductivity. The aluminum tube and mylar sheath thus formed the two plates of a capacitor microphone. The biasing scheme is also given in Figure 4.

Due to the large amount of room noise (resulting from handlers, vacuum pumps, teletypes, conversation, etc.) as well as electrical noise in the laboratory, shielding was incorporated around the cell. An aluminum electrical noise shield comprised of a 10 cm X 10 cm X 55 cm rectangular chassis was placed around the cell to protect the high resistance biased capacitor

microphone from electrical noise. The chassis was wrapped with 2.5 cm thick foam rubber. The ends of the cell extending out of the chassis were wrapped with 1.2 cm thick soft rubber. The cell was positioned by stands sitting on a 2.5 cm thick foam rubber.

For detection limit studies, a flowing gas stream with very low concentration levels of the analyte species was needed. A dynamic gas mixing module was used in this study in which small flow rates of a gas mixture of the analyte species of interest was introduced into a larger flowing pure air stream. All plumbing consisted of one-eighth inch OD copper tubing and one-eighth inch "Swage-lok" fittings. Calibrated rotameters were used to set the flow rates of the analyte mix (using a 200 cc/min rotameter) and the pure air stream (using a 3,000 cc/min rotameter). The air and analyte gas stream came together using a "T" fitting followed by a mixing coil consisting of eight turns of one-eighth inch copper tubing with a turn radius of 2 cm. By setting relative flow rates using needle valves, the analyte mixture could be effectively diluted up to a factor of 500. The validity of this mixing procudure was verified by GC analysis where several diluted samples of a 800 ppm ethylene and freon-12 gas mixture were collected in gas sampling bulbs and subsequently analyzed.

A calibrated 3.7 ppm ethylene and freon-12 gas mixture in air was made using the following procedure. A 55 cubic foot nitrogen tank was evacuated. The contents of 125 ml gas sampling bulbs of pure freon-12 and ethylene were added by suction to the tank which was filled to 800 psi with pure air. The contents of this tank was added to another tank (initially containing 15 psi of pure air) to a total pressure of 25 psi. This second tank was then filled with pure air to a pressure of 800 psi. The contents of the second tank was calibrated against an analyzed 1 ppm ethylene in air standard

(Matheson Gas Products, Newark, CA) using both optoacoustic and GC analysis.

The windowless non-resonant cell data was compared with one cell of a differential cell pair consisting of a 2.5 cm long by 1.27 cm internal diameter cell containing 2.5 cm x .2 cm thick ZnSe windows at each end of the two cells. The two cells were separated by a 2.5 cm x .2 cm thick antireflection coated germanium window. The microphones used in both cells were Knowles BW-1789 (Knowles Electronics, Franklin Park, Ill.) microphones with and active area of 0.75 cm. Their sensitivity was rated as -55 db referenced to 1 volt per microbar.

The optoacoustic spectrometer system used in this study consisted of a CO_2 laser (2.7 meter cavity length, 2.5 meter plasma tube) with a 75 1/mm grating capable of outputing over 10 watts at over 70 lines in both CO_2 lasing transitions. No mode control was used with this laser, typically the mode control was very poor resulting in the output being split between a few to several modes. A KT-2010 pyroelectric detector (Laser Precision, Yorkville, NY) was used for relative power measurements after first passing the beam through a diffuser. A Par 5101 and Par 126 (PAR-EGG Corp., Princeton, NJ) lockin amplifier, are used to measure the signal from the optoacoustic cell and pyroelectric detector respectively. A PAR 125 mechanical chopper was used to chop the laser beam. Optoacoustic scans were output on a linear 225 strip chart recorder (Linear Instruments, Irvine, CA). A calibrated General Radio 1565-B (General Radio, Concord, MA) sound pressure meter (calibrated with a General Radio 1567 calibration source) was used for laboratory background sound pressure (level) readings.

Results and Discussion

The frequency response of the windowless cell was determined by measuring the optoacoustic signal of a 3.7 ppm ethylene mixture continuously flowing through the cell. As shown in Fig. 5, the frequency response of this cell had a distinct peak near 250 Hz. These data were corrected for the 1/f frequency response inherent in the optoacoustic technique by normalizing all data relative to the measured signal at 990 Hz. Since longitudinal resonance modes in this windowless cell cannot be excited and the first radial and azimuthal modes would not appear except at very high chopping rates (above 15 kHz), this peak is clearly due to resonance of the microphone itself. Resonance peaks of capicator microphones are common,[11] manufactures of commercial capicator microphones go to great effort to achieve flat frequency re_ponse when designing these microphones. However in optoacoustics, microphone resonance peaks can be used to advantage.

The acoustic room noise spectrum measured with the windowless cell is shown in Fig. 6. No special effort was made to reduce the room acoustic noise during this and all subsequent studies. The sound pressure level (SPL) near the windowless cell was measured at 78 db with C weighting (flat response) and 68 db using A weighting (increased low frequency roll off).

Assuming room noise is the dominant noise source, the optimum chopping frequency is that which maximizes the signal to acoustic room noise (S/N) ratio. From Fig. 7 it is clear that the net S/N is maximized near the

resonance peak at 250 Hz.. Given the selection of discrete chopper speeds available, a chopping rate of 260 Hz was used in all subsequent studies.

The windowless cell's ability to supress background signals is most dramatically demonstrated by comparing optoacoustic scans taken using a conventional cell (one cell of the differential cell pair) vs. that of the windowless cell. Figure 8 clearly demonstrates that the background signal (due to wall absorption) is significantly less than that of the conventional cell by comparing scans of a 3.7 ppm mixture of ethylene and freon-12. For example, the signal to background ratio at the ethylene absorption peak (the P14 laser line of the 100 transition) is 150.1 for the windowless cell and 4.8 for the conventional cell. Expressed as an equivalent absorption, the background level for the windowless and conventional cell is 7.7×10^{-7} cm^{-1} and 2.5×10^{-5} cm^{-1} respectively.

A study was initiated to determine the variability of the cell wall background during multiple background scans and to determine the background sensitivity to cell position in relation to the laser beam passing through it. It was found that the background wall absorption could be minimized by optimizing the position of the cell. Cell position changes of less than one degree had negligible effect on the background signal (a maximum of a 10% change in background level). However with the cell adjusted several degrees from optimum the background could be increased by a factor of 5. This is not surprising considering that the laser beam was

actually reflecting twice from the cell wall while transversing the cell under these conditions. It was not possible to raise the background to a level comparable to that observed using the conventional cell even with multiple reflections of the laser beam through the cell cavity.

Once the cell position was optimized, multiple background scans were recorded to determine the variability of the background signal measured at the laser line giving peak background signal at each of the 4 CO_2 lasing branches. The background signal was ratioed with the pyroelectric laser power signal. The results of one such study is shown in Table I, where the results of 4 background scans are tabulated. The relative standard deviation between multiple scans was between 7.4% to 24.3%, depending on the particular branch observed. The uncertainty in the background level sets the detection limit capability of this cell since the accuracy of any background subtraction scheme is only as good as the accuracy in determining the background level. Assuming that the uncertainty of the background is the major noise source, detection limits expressed as an equivalent absorption are between 1.5×10^{-7} cm^{-1} and 5.9×10^{-7} cm^{-1} at 3 standard deviations.

The variance in the background is the sum of the variances of room noise added on top of the background and the variance of the background itself. The magnitude of the room noise, measured with the laser tuned to a non-lasing position, was found to be at a level equivalent to 10% of the background signal. The variance of the background level itself could not be directly decoupled from the room noise. However given the magnitude of the room noise signal on the background, it appears to be the dominant source of variance on the background signal.

Although the detection limit should be defined by the uncertainty of the background, a detection limit study was initiated to test this conclusion under actual experimental conditions. From the literature it appears that many authors use measured detection limits for one gas at one laser line and extrapolate these limits to other gases given a knowledge of the ratio of absorption coefficients of the two gases. It is the opinion of these authors that detection limits at more than one line (perferably using more than one line for at least two gases) should be measured using the same procedures that would be employed under actual analysis conditions. This should give a better measure of the detection limit capabilities of the optoacoustic system when employed for real world analysis.

In this study detection limits of an ethylene and freon-12 gas mixture were measured at 4 laser lines using 2 lines to determine the detection limit of each gas. Two of these lines were in the P100 branch, one line was in the R100 branch and the fourth line was in the R020 branch of the CO_2 laser. The laser line designation and absorption coefficient of the respective gas which absorbs at each laser line is shown in Table II. The desired concentration of the ethylene and freon-12 gas mixture was generated from a standard 3.7 ppm ethylene and freon-12 mixture using the dynamic dilution technique described previously. It was determined that the optoacoustic response of the cell was independent of flow rate from 100 cc/min to 3000 cc/min. However it was observed that the background acoustic noise increased slightly at flow rates above 1500 cc/min to a maximum of 2.5 times the ambient background noise at a

flow rate of 3000 cc/min. The noise was essentially independent of flow rate between zero flow and 1500 cc/min.

The procedure for performing detection limit studies envolved running a background scan to determine the optoacoustic signal at the 4 laser lines used in this study. The optoacoustic signal was corrected for laser power by dividing all optoacoustic signal data with the data value taken from the laser power monitor channel. The cell was flushed with the required ethylene and freon-12 gas mixture diluted with pure air, and while maintaining this flow rate a new scan was run. The signal at the 4 laser lines was measured and normalized for laser power. The previously determined background signal was subtracted from this value. This procedure was repeated at increasingly diluted gas concentrations.

A curve of normalized signal vs. concentration at each of the four laser lines is given in Figures 9 thru 12. From these curves the detection limits at each wavelength were determined. The criteria used to define the detection limit was to find the concentration value at the intersection of the flat portion and the extrapolated linear portion of the working curve. This detection limit was essentially the same as that predicted (using a two to one S/N criteria) from signal to noise measurements at a concentration level approximately 5 times greater than that at the detection limit. Detection limits are summarized in Table III. Detection limits are given both as concentrations and the equivalent absorption at that concentration. Note that the equivalent detection limit absorption defined by actual working curves is generally similiar to those calculated from variance measurements of the background signal (see Table I). Each equivalent absorption value should be identical.

The poor value determined for ethylene at the R24(100) line can be attributed to water vapor contamination since water vapor does have relatively large absorption in this region. Since the laser power at the Freon-12 R20 line in the 020 transition was 1/5 that of the line in the P100 transition, the equivalent absorption value at the R20(020) line was correspondingly larger than the value at the P34(100) line. The average absorption detection limit at the P100 branch is approximately 1.3×10^{-7} cm^{-1} which is similar to that obtained from a differential cell in the focused laser beam geometry used in this laboratory. All detection limit data used a 10 sec. time constant setting on the lockin amplifier which was the maximum time constant compatable with the scanning mode of data collection.

The optoacoustic technique is observed to be linear over a wide concentration range as shown in Figure 13. These data were taken using ethylene in the P14 line of the 100 transition. Note that the optoacoustic signal vs. concentration is linear over 4 orders of magnitude. However there is considerable deviation from linearity at concentrations above 100 ppm due to the considerable loss of laser power through the long path length cell. For instance, at a concentration level of 200 ppm ethylene, laser power should be attenuated by two. Measurements of laser power with and without a 200 ppm ethylene sample flowing through the cell confirmed this.

To examine the wall adsorption contamination problem of the windowless vs. the differential cell, both cells were contaminated with methanol vapor. Methanol, as well as many other polar compounds, can adsorb strongly on the walls of metallic cells.

Methanol vapor was added to the one cell of the differential cell pair at a concentration of 0.1% and an optoacoustic scan was recorded. The cell was flushed with 1500 cc/min of pure air and after a specified flush period, the cell was sealed and a new optoacoustic scan was recorded. This was repeated several times giving an equivalent flush time of 35 minutes. Methanol vapor was similiarly added (0.1%) to the windowless cell and the cell ends temporarily sealed for 3 minutes to allow methanol wall adsorption to equilibrate. The laser was tuned to a methanol absorption peak (the P20-020 line) and the optoacoustic signal was recorded continuously after starting a 1500 cc/min flush in the cell.

The results of this study are shown in Figure 14. Note that the signal from the windowless cell became undetectable after 3.5 minutes. However methanol could still be detected after 35 minutes in the differential cell. After 4 minutes of flushing in the windowless cell the flush was stopped at which time a methanol signal started to reappear. This demonstrates that the windowless cell is not less prone to adsorption effects than conventional cells but with continuous flushing through the analysis section of the cell, the analyte molecules released from the cell walls become significantly diluted in the flowing stream.

Conclusion

It has been shown that the windowless non-resonant cell allows flow through operation suitable for stream monitoring while minimizing cross contamination from previous samples. This approach to cell construction directly eliminates window noise in a manner which is independent of

laser mode control and focusing. It was also shown that these advantages are maintained while allowing the measurement of gas mixtures at a concentration level less than 10 ppb.

Acknowledgement

This research was partially supported by the Office of Naval Research and by an Alfred P. Sloan Foundation Research Fellowship awarded to M. B. Denton.

References

1. L. B. Kreuzer, J. Appl. Phys. 42, 2934 (1971).
2. M. J. Colles, N. R. Geddes and E. Mehdizadeh, Contemp. Phys. 20, 11 (1979).
3. K. F. Luft, Zeit. Tech. Physik. 24, 97 (1943).
4. T. F. Deaton, D. A. Depatie and T. W. Walker, Appl. Phys. Lett. 26, 300 (1975).
5. P. D. Golden and K. Gotto, J. Appl. Phys. 45, 4350 (1974).
6. R. D. Kamm, J. Appl. Phys. 47, 3550 (1976).
7. C. W. Bruce, B. Z. Sojka, A. G. Hurd, W. R. Walkins, K. O. White and Z. Derzko, Appl. Optics 15, 2970 (1976).
8. E. Kritchman, S. Shtrikman and M. Slatkine, J. Opt. Sco. Am. 68, 1257 (1978).
9. J. G. Parker, Appl. Opt. 12, 2974 (1973).
10. L. Rosengren, Appl. Opt. 14, 1960 (1975).
11. H. W. Tremaine, Audio Encyclopedia, (Howard W. Sams, Indianapolis, IN, 1979), 8th ed., Chapter 4, p. 159.

Figure Captions

Fig. 1. Typical components of an optoacoustic spectrometer.

Fig. 2. Typical differential cell arrangement.

Fig. 3. Theory of signal generation in the windowless non-resonant cell. The current pressure wave in the center of the cell is contained by the previous pressure wave which has moved toward both ends of the cell.

Fig. 4. Schematic and biasing scheme of the windowless non-resonant cell.

Fig. 5. Normalized frequency response of the windowless non-resonant cell.

Fig. 6. Acoustic room noise spectrum measured with the windowless non-resonant cell in the laboratory where all subsequent measurements were taken.

Fig. 7. Net signal/noise vs. frequency of the windowless cell.

Fig. 8. Scan of the background and 3.7 ppm freon-12 and ethylene gas mixture taken with the windowless non-resonant cell (top scan) and conventional cell containing windows.

Fig. 9. Normalized optoacoustic signal vs. concentration for freon-12 at the P34(100) CO_2 laser line.

Fig. 10. Normalized optoacoustic signal vs. concentration for ethylene at the P14(100) CO_2 laser line.

Fig. 11. Normalized optoacoustic signal vs. concentration for ethylene at the R24(100) CO_2 laser line.

Fig. 12. Normalized optoacoustic signal vs. concentration for freon-12 at the R20(020) CO_2 laser line.

Fig. 13. Extended working curve of ethylene at the P14(100) CO_2 laser line taken with the windowless non-resonant optoacoustic cell.

Fig. 14. Comparison of the rates of the removal of methanol contamination for the windowless non-resonant and differential cell.

TABLE I. Relative background level at the center of the four CO_2 lasing bands from four consecutive scans.

Scan #	Laser Branch:	P100	R100	R020	R020
1		1.70	1.2	2.15	3.20
2		1.45	1.21	2.35	2.90
3		1.81	1.90	2.85	2.65
4		1.51	1.78	2.30	2.92
	Average:	1.62	1.52	2.41	2.91
	Std. Dev.:	0.17	0.37	0.30	0.22
	RSD:	10.4%	24.3%	12.4%	7.4%

TABLE II. Absorption coefficients of Freon-12 and Ethylene at the 4 CO_2 laser lines used to determine detection limits.

Laser Line	Absorbing Gas	Absorption Coefficient $(atm.\ cm)^{-1}$
P14(100)	Ethylene	29.1
P34(100)	Freon-12	21.0
R24(100)	Ethylene	5.3
R20(020)	Freon-12	9.1

TABLE III. Detection limits of Ethylene and Freon-12 at the laser lines used in the detection limit study.

Laser Line	Gas	Detection Limit (ppb)	Equivalent Absorption
P14(100)	Ethylene	5.0	1.5×10^{-7} cm^{-1}
P34(100)	Freon-12	5.5	1.1×10^{-7} cm^{-1}
R24(100)	Ethylene	90.	4.9×10^{-7} cm^{-1}
R20(020)	Freon-12	90.	8.2×10^{-7} cm^{-1}